# QUALIFICATION OF A RELAP5-3D© SYSTEM CODE NODALIZATION OF EBR-II

**A. Del Nevo**
ENEA
Camugnano, 40032, Brasimone, Italy
alessandro.delnevo@enea.it

**E. Martelli**
UNIROMA
Università "La Sapienza", Roma, Italy
emanuelamartelli@hotmail.it

**ABSTRACT**

ENEA is setting up, applying and validating numerical models and an integrated multi-physics approach, based on existing codes and aimed at supporting safety analysis of liquid metal Gen. IV fast reactors. The paper provides an outline of the activity and it is focused on qualification of a three-dimensional thermal-hydraulic model of EBR-II primary and secondary systems using the system code RELAP5-3D©. The nodalization models one by one the fuel assemblies of the core and of the extended core of the reactor for an easy and efficient coupling with a 3D neutron kinetic code. The paper presents the qualification of the nodalization based on the EBR-II test SHRT-17. The analysis of the experimental data, the identification of the thermal-hydraulics phenomena observed in the tests are the basis for assessing the code performances and for discussing its limitations.

**KEYWORDS**
Fast Reactors, System Thermal-hydraulics, EBR-II, RELAP5-3D©

## 1. INTRODUCTION

The International Atomic Energy Agency (IAEA) established a Coordinated Research Project (CRP) on EBR-II Shutdown Heat Removal Tests (SHRT) for supporting the validation of simulation tools and models for the safety analysis of Liquid Metal Fast Reactors (LMRs) [1]. The project aims at improving design and simulation capabilities in fast reactor neutronics, thermal hydraulics, plant dynamics and safety analyses through benchmark analysis (coordinated by the Argonne National Lab) of the SHRT-17 protected loss of flow and SHRT-45R unprotected loss-of flow tests from the EBR-II SHRT program. The SHRT-17 is a protected loss of flow, used to demonstrate effectiveness of natural circulation cooling characteristics. Starting from full power and flow, both primary loop and intermediate loop coolant pumps are simultaneously tripped and the reactor is also scrammed to simulate a protected loss-of-flow accident. In addition, the primary system auxiliary coolant pump that normally had an emergency battery power supply was turned off.

In this framework, ENEA has set up, applied and is validating an integrated multi-physics approach, based on existing codes, for supporting the design and the safety analysis of Gen. IV liquid metal fast reactors. [2][3].

The main objective of the activity is the validation of RELAP5-3D© system code in simulating liquid metal fast reactor designs, comparing best-estimate thermal-hydraulic system code calculations to experimental data and identifying RELAP5-3D© code limitations and the source of uncertainties [4]. In order to achieve this objective, the activity aims at improving the understanding of the thermal-hydraulic processes and phenomena observed in EBR-II test and at developing reliable approach for the application of thermal-hydraulic system codes in safety analysis of new generation fast reactors system including the coupling with CFD and NK codes.

The paper provides an outline of this activity (funded by the Ministry of Economic Development) and it is focused on the development and the validation of a three-dimensional thermal-hydraulic model of EBR-II primary and secondary systems using the system code RELAP5-3D©. The nodalization models one by one the fuel assemblies of the core and of the extended core of the reactor for an easy and efficient coupling with a 3D neutron kinetic code. The analysis of the experimental data, the identification of the thermal-hydraulics phenomena observed in the test SHRT-17 are the basis for assessing the code performances and for discussing its limitations.

## 2. THE MULTI-PHYSICS APPROACH

In the framework of the IAEA CRP EBR-II Shutdown Heat Removal Tests (SHRT), ENEA has set up, applied and is validating an multi-physics approach, based on existing codes, for supporting the design and the safety analysis of Gen. IV liquid metal fast reactors (Fig. 1). The approach [3] is based on existing well-qualified nuclear codes, interacting as depicted in Fig. 1: ERANOS 2.1 [5] and MCNP6 [6] codes for (static) deterministic and stochastic neutron transport calculations, SCALE [7] package for cross section generation; PHYSICS [8] neutron kinetic package for 3D core power distribution calculations in steady state and in transient, coupled with RELAP5-3D©; RELAP5-3D© for system analysis; computation fluid dynamic code ANSYS CFX 13 [9] for 3D local simulations; and TRANSURANUS [10] code for fuel pin performance simulations (not employed in the benchmark activities). Neutron physics codes will be applied for simulating the test SHRT-45r, which is an unprotected transient where the neutronic feedbacks have a crucial role. The RELAP5-3D© notalization, qualified against the test discussed in this paper, is used for the thermal-hydraulic calculation of the transient. On the opposite, ANSYS CFX-13 is used to perform a detailed simulations of the experimental sub-assemblies XX09 and XX10 for the tests SHRT-17 and SHRT-45r. The three dimensional simulation provides detailed description of the flow path and temperature distribution inside the fuel assembly and in the sub-assembly thimble and it will benefit of the large number of thermocouple installed in the bundle. Description of this activity is beyond the scope of the present paper. However preliminary results are reported in Ref. [3].

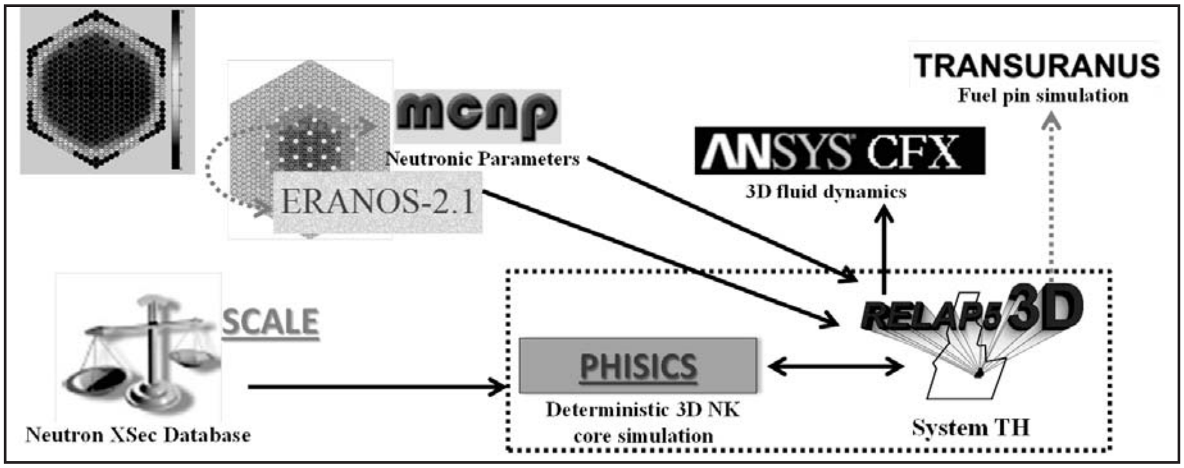


**Figure 1. Chain of codes proposed.**

## 3. OVERVIEW OF EBR-II

The Experimental Breeder Reactor II is a sodium cooled reactor located in Idaho. It was designed and operated by Argonne National Laboratory for the US Department of Energy. Operation began in 1964 and continued until 1994. EBR-II was rated for a thermal power of 62.5 MWt with an electric output of approximately 20MWe [11].

All primary system components were submerged in the primary tank. An argon cover gas was maintained over the surface of the sodium in the primary vessel to minimize the opportunity for air to contact the sodium. The primary sodium circuit had three pumps: two main and one electromagnetic pump. The main primary centrifugal pumps pumped 485 kg/s of sodium from the pool to the inlet plena, through the two identical sets of reactor inlet piping. The lower inlet plenum received coolant from the two low-pressure inlet pipes and fed the core blanket region. The upper inlet plenum received sodium from the two high-pressure inlet pipes, in the high-pressure inlet plenum sodium was distributed to the central core region. Sodium from these two inlet plena was provided to the reactor assemblies and then discharged into the common upper plenum.

Coolant left the upper plenum through the reactor outlet pipe and entered into the Z-Pipe, where the auxiliary EM pump was located. Sodium flowed off from the Z-Pipe and entered the shell side of the intermediate heat exchanger (IHX), which was in charge to remove the heat from the primary system towards the steam generator. The IHX was a tube-and shell design with single-wall straight tubes and was operated in the counter flow mode.

Colder sodium from the IHX was finally discharged into the primary sodium tank before entering the primary sodium pumps again [11].

The EBR-II reactor core accommodated 637 hexagonal assemblies. The assemblies were located into three regions: core, expanded core and outer blanket (OB). The central core comprised 61 assemblies in the first five rows. Two positions in Row 5 contained the in-core instrument assemblies, identified as XX09 and XX10. In case of test SHRT-17, the Rows 6 and 7 (i.e. 66 assemblies), fed by the two high-pressure inlet pipes, belonged to the expanded core region. The outer blanket region comprised the 510 assemblies in Rows 8-16, which were either blanket or reflector assemblies [11].

The metallic fuel is fabricated in U-5Fs alloy. The fuel elements, placed inside the cladding, were sodium bonded.

## 4. SHRT-17 EXPERIMENT

SHRT-17 was loss of flow test used to support LMR plant design and to demonstrate effectiveness of natural circulation cooling characteristics. The experimental test starts with EBR-II in nominal steady state conditions, thus at full power and flow. The initiating events are the trip of the primary coolant pumps and of the intermediate-loop pump. The reactor was instantaneously scrammed. The reduction in coolant flow rate caused reactor temperatures to rise temporarily to high, but acceptable levels, as the reactor safely cooled itself down at decay heat levels by natural circulation. The test stops after 15 minutes without any operator action any system intervention. Three phases and related phenomena are identified in the transient, as discussed in section VI. They are:

- Phase 1 – effective core cooling by MCP caostdown (0 – 10s): from initiating events to fuel cladding starts to rise;
- Phase 2 – primary system energy increases and temperatures rise (10 – 100s): from end of Phase 1 up to maximum fuel temperature in the core;
- Phase 3 – buoyancy forces effective in removing energy from the core, long term cooling in natural circulation (100 – 900s): from end of Phase 2 up to end of transient.

## 5. RELAP5-3D NODALIZATION

EBR-II nodalization (Fig. 2) has been carried out by RELAP5-3D©V4 code [12]. The nodalization can be divided into two parts:

1. The coolant system, that includes: the pool region, the lower and the top part of the pool; the major components in the primary sodium circuit: pumps, high and low pressure flow lines, throttle valve; the Z-Pipe and the intermediate heat exchanger, primary and secondary side.
2. The reactor region, that includes the reactor vessel, including the lower plenum, the upper plenum and the core bypass; the core subassemblies, divided in the central core region (driver subassemblies) and outer blanket region (reflector and blanket subassemblies).

### 5.1. Coolant system model

The pool region is modeled with a 3D component (i.e. MULTID), see Fig. 2a. The number of azimuthal meshes have been chosen in order to represent with the least number of volumes the real position of the pumps, the inlet of the pipes and of the IHX. The axial meshes of the pool region have vertical lengths equal or multiple with respect to reactor region, pipes and IHX. Each component in the pool is positioned as in the real 3D geometry.

The pumps have been modeled with a PUMP component. The homologous curves are implemented using the characteristic curves provided for the pump, see Ref. [2]. The high and low-pressure flow lines have been modeled with 1D components (i.e. PIPE and BRANCH components). The reactor outlet pipe, or Z-Pipe, connects the reactor zone and the IHX. It has been also modeled with a PIPE component. The connections from the reactor vessel to the Z-Pipe and from the Z-Pipe to the pool have been modeled with single junctions. The secondary side of the IHX is modeled with RELAP5components for setting the boundary conditions according with reactor design (i.e. pressure at the outlet and coolant temperature and mass flow rate at the inlet) and 1D components. The heat exchange with the primary system is modeled with RELAP5 heat structures. In particular, the thermal coupling is in concurrent direction (i.e.

primary system and central tube) and counter-current direction (i.e. primary system and tube bundle).

### 5.2. Reactor core model

A 3D component (MULTID) represents the reactor vessel: the lower plenum, the upper plenum and the core bypass (Fig. 2b).

The azimuthal subdivision is made in order to represent the real position of the inlet and outlet of the pipes and the symmetry of the core. The axial nodes have lengths equal or sub-multiple with respect of the meshes of the 3D component representing the pool region.

The core bypass is connected with the high pressure coolant plenum in the bottom and the upper plenum on the top. It is thermally coupled with the FA, through the wrappers and the pool system through the neutronic shield.

The reactor core is divided into two main parts, according with the specifications of Ref. [11]:

1. the assemblies of the central core and the expanded core regions, the first 7 rows, fed by the high pressure plenum, are modeled one by one, according with the geometrical specifications.
2. the outer blanket region, fed by the low pressure plenum, is modeled with 24 equivalent PIPE components, grouping separately reflector and blanket assemblies, according with azimuthal configuration.

The model of each assembly (Fig. 2c) in the core regions is rather detailed to represent all relevant geometric characteristics and positions: BAF, TAF and thermocouples. Fuel assembly orifices have been setup on the basis of mass flow rates data and overall dynamic pressure drops in nominal steady state.

### 5.3. Main features of the nodalization

The main features of RELAP5-3D© input deck adopted are:

- Recommended common rules involving characteristic dimensions, flow path area, elevations, heat structures and capacities have been taken into account from the EBR-II benchmark data [4].
- Bypass is modeled according to geometric specifications, when available, and mass flow data in steady state.
- A sliced approach is applied at all systems (i.e. coolant system, reactor core).
- The elevations of the different parts of the plant are maintained in the nodalization.
- Dimension of nodes is set-up according with the expected spatial temperature gradients, relevant geometrical features of the systems and measurement points constraints.
- The node to node ratio is kept uniform, as much as possible, with reference maximum ratio of 1.2 between adjacent sub-volumes.
- The roughness is set 3.2e-5 m with the exception of the core region, where is set 1.0e-6 m as consequence of the nodalization qualification as reported in Ref. [3] and [13].
- The standard REALP5 wall friction correlations (i.e. laminar and turbulent regions) are modified with Cheng and Todreas formulations to represent wire wrapped rod bundle with optionally form loss coefficient with a Reynolds dependence [14], [15].
- K-loss coefficients in junctions have been evaluated or estimated on the basis of geometries, when available.

- Standard RELAP5 liquid metals correlations are used for convective heat transfer for non-bundle and bundle zones, described in Refs. [14] and [17].

A scheme of the nodalization is represented in Fig. 2. A detailed description of the nodalization is in Refs. [3] and [13].

## 5.4. Modeling changes for open calculation

The open simulations of the test SHRT-17 are carried out with few modifications in the input deck:

- The pressure drops of the primary system are set-up according with the experimental results of the test. Dependence of energy loss coefficients from Re number is taken into account to improve the prediction of the mass flow rate in the sub-assembly.
- The azimuthal orientation of the core with respect to the high and low pressure line connections has been corrected as in the real configuration, thanks to up-dated information delivered by the benchmark coordinators.

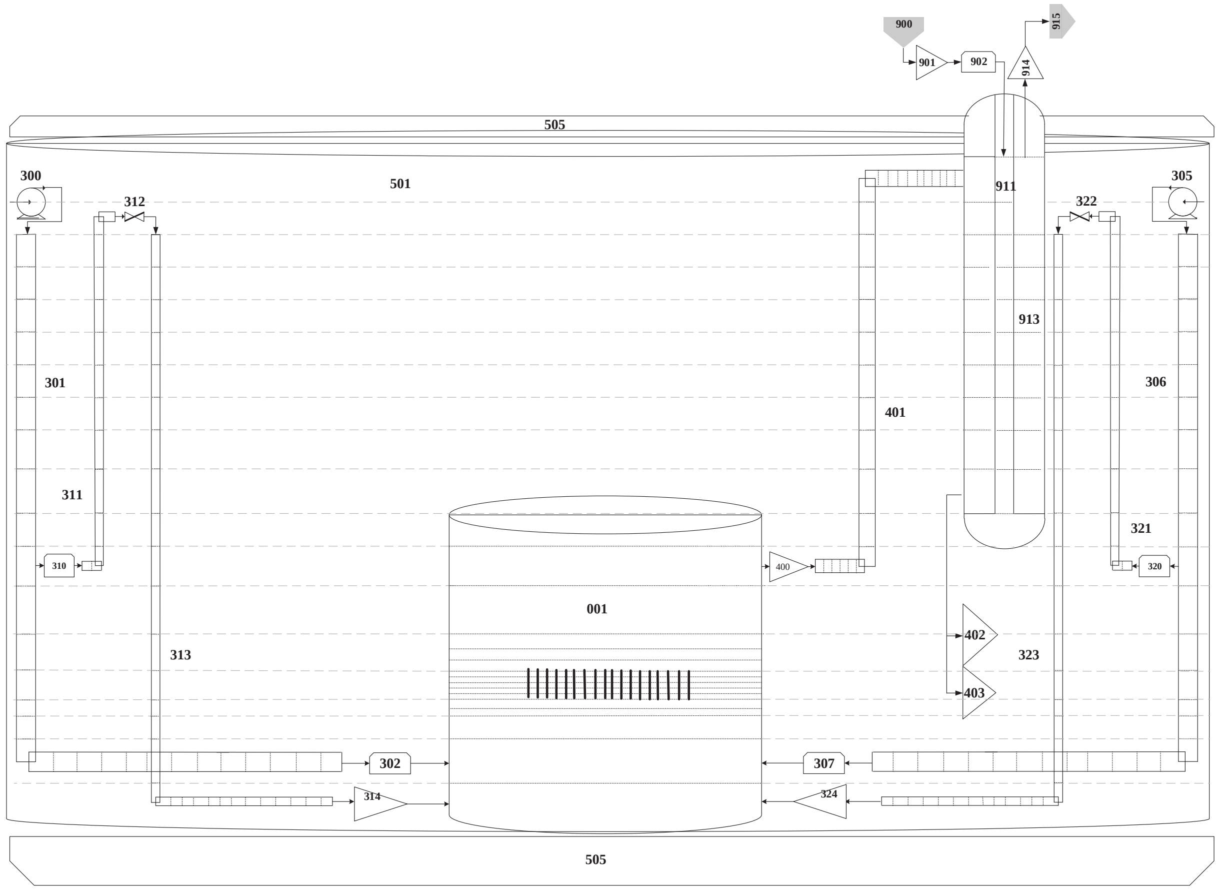


*(a) Overall nodalization*

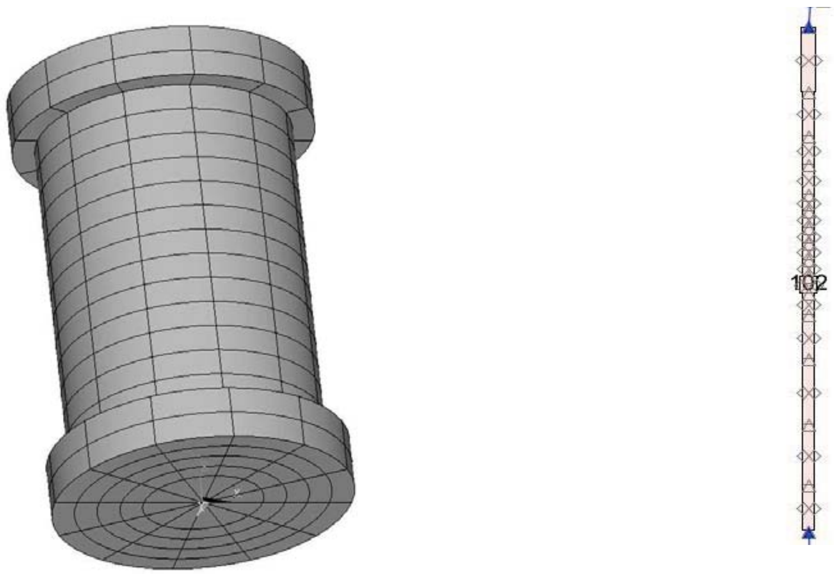


*(b) Reactor vessel component* *(c) Experimental sub-assembly X406 coordinate [2,B1]*

**Figure 2. EBR-II SHRT-17 RELAP5-3D nodalization.**

## 6. QUALIFICATION OF EBR-II NODALIZATION

The results of two code simulations are presented: the blind calculation, performed on the basis of initial and boundary conditions delivered to the benchmark participants, and the open calculation, after the availability of the experimental data trends.

The mass flow rate distribution in the core sub-assemblies (i.e. core, extended core and blanket/reflector zones) has been set up using steady state data in isothermal conditions released to the benchmark participants[11]. These data provides mass flow rates in core sub-assemblies at rated pump operation. Detailed sub-assembly power distribution was also provided to benchmark participants with the reactor core at full power. Then, total core fission and decay heat powers versus time were given in the specifications [11]. The other boundary conditions used to set up the code simulations of SHRT-17 test were: MCP speeds versus time; IHX secondary side mass flow rates and temperature versus time.

The initial conditions of the experiment and at the end of the steady state calculations are compared in Tab. I. Steady state and initial conditions are achieved accordingly with the specifications for blind and open simulations. Few minor deviations are observed among the code results and the experimental data.

The correct prediction of the initial test conditions requires a correct modelling of the coolant pump characteristics, overall set-up of the pressure drop in the system and, considering the nodalization features, of the pressure drop distributions assembly by assembly. The heat transfer correlations in core bundle zone and IHX benefits of geometrical data inside of the range of validity of REALP5-3D© correlation[17]. However, the IHX primary system has a P/D equal to 1.3, thus an (acceptable) underestimation of Nusselt is expected. This effect is negligible, considering the layout of EBR-II primary system and the large thermal inertial of the pool, and the short duration of the test.

The comparison of the resulting sequences of main events and related phenomena is reported in Tab. II. Selected experimental and calculated parameter trends are reported below and discussed. Three phases are identified in the transient. The relevant TH phenomena common to all phases of the transient are: pressure drop at geometrical discontinuities; wall to fluid friction; heat transfer in core; heat transfer in passive structures and heat losses; pool thermal hydraulics in the tank; multidimensional coolant temperatures and flow distributions; and conduction in fluid and structures. Specific phenomena of each phase are reported in Tab. II.

The initiating events of the test are the primary pumps and the intermediate pump trips (Phase 1). The reactor SCRAM occurs and the transient evolves without any system intervention or any operator/external action, thus such as a station blackout. The core temperatures decrease for about 10 s (9 seconds considering the cladding temperatures at TAF of sub-assembly XX09, reported in Fig. 3), because the sharp decrease of nuclear fission power and the mass flow rate (Fig. 4), with the pump coasting-down, is above 30% of initial value. Correct prediction of this phase is mainly connected with the energy distribution in the core structures, the thermal inertia and, then, the evaluation of the pressure drop in the system (i.e. dominated by the sub-assembly inlet orifices and friction losses in wire wrapped fuel bundle) and the pump coastdown. The main parameters trends of blind and open simulations are satisfactory during this phase.

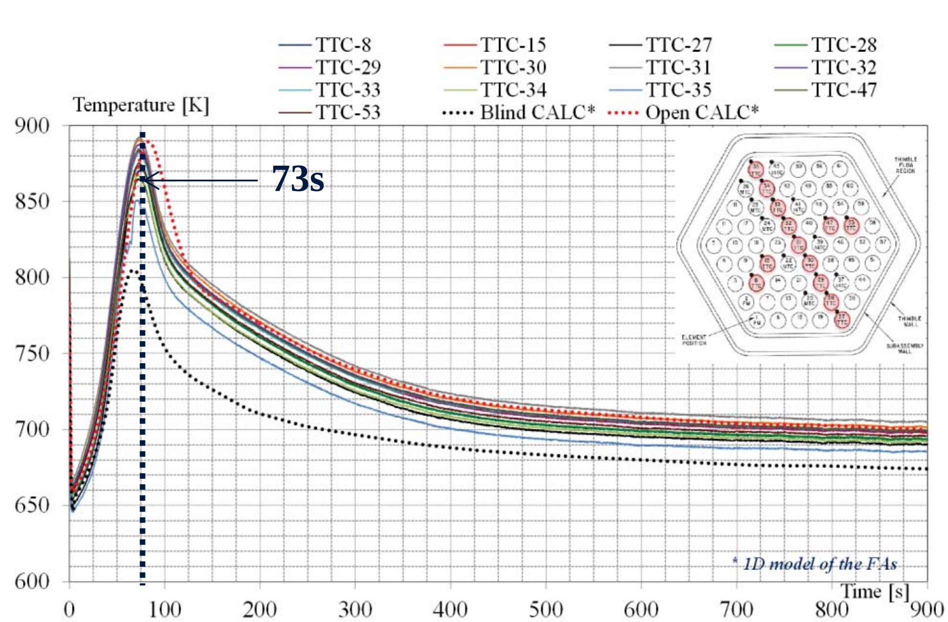


**Figure 3. XX09 cladding T at top of active core**

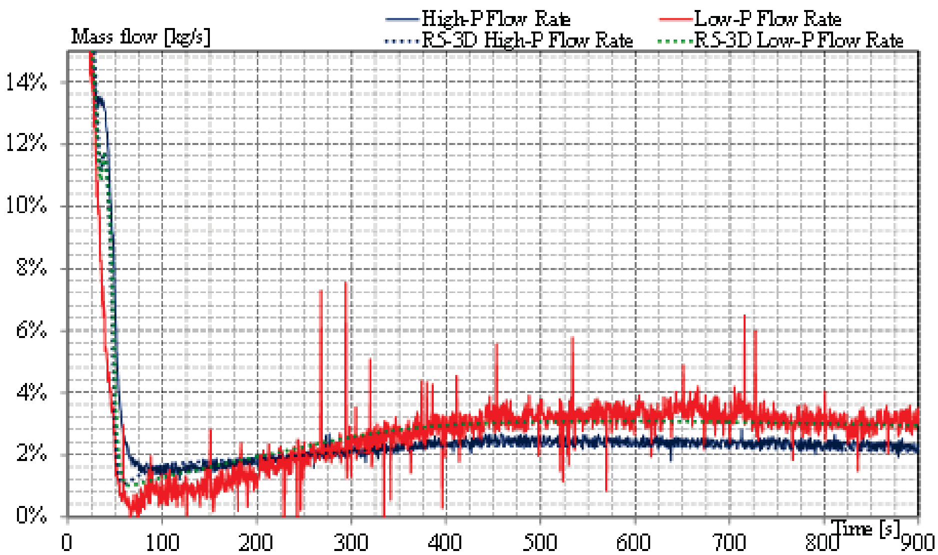

**Figure 4. High and low-pressure mass flow rates, loop #2**

When the coolant pump flow rate decreases below 30% of nominal mass flow rate, the unbalance between the total core power (fission and decay heat) and the energy removed by the primary coolant flow causes a sharp increase of cladding and coolant temperatures in the sub-assemblies (phase 2). The maximum cladding temperatures experienced by the experimental sub-assemblies XX09 and XX10 at top of core active fuel are observed at 73 s and 96 s, respectively (see Fig. 3 and Fig. 5). Code predictions are driven by the pump inertia, the pressure drops calculated in the sub-assemblies inlet orifices and in the wire wrapped fuel bundles. It is expected that the REALP5-3D© has the capability to model the Reynolds dependent energy loss coefficients of these geometries, with some limitations in the laminar region, as discussed in Ref. [16]. The timing and the rates of coolant and cladding temperature increases in the core are qualitatively and quantitatively well predicted in the code simulations (i.e. blind and open). As regards as, the peak of cladding and coolant temperatures of fuel sub-assemblies, the blind simulation is affected by an underestimation. This is connected with the faster mass flow rate increase, following the pumps coastdown end, and with the flow stabilization to an higher value. It is explained with the inadequacy of the modelling the inlet sub-assembly orifices with the Reynolds independent energy loss coefficients, used for the blind calculation.

The open calculation evidenced an excellent simulation of the mass flow rates measured in the high and low pressure lines (Fig. 4), as well as of the mass flow rates in the available experimental sub-assemblies XX09 and XX10 (not reported). Some quantitative differences are observed and hereafter discussed. Considering that the mass flow rates are correctly predicted, the coolant flows from the high and low pressure feeding pipes towards the corresponding lower plena, delivering the sodium towards the different sub-assemblies. In this zone, complex three dimensional coolant flow distribution is roughly simulated by the coarse MULTID component of RELAP5-3D. Then, once the natural circulation is the prevailing driving force of the primary flow, the thermal conductivity in the core thermal structures and in the fluid becomes relevant. The reference blind and open calculations do not account for the axial thermal conduction of the heat structures (i.e. only radial conductions is calculated by the code). However, the code has the capability to calculate the axial conduction in the heat structure, but it does not have the same capability for the conduction in the fluid. This would result in a conservative prediction of the code simulations with respect to temperatures of heat structure.

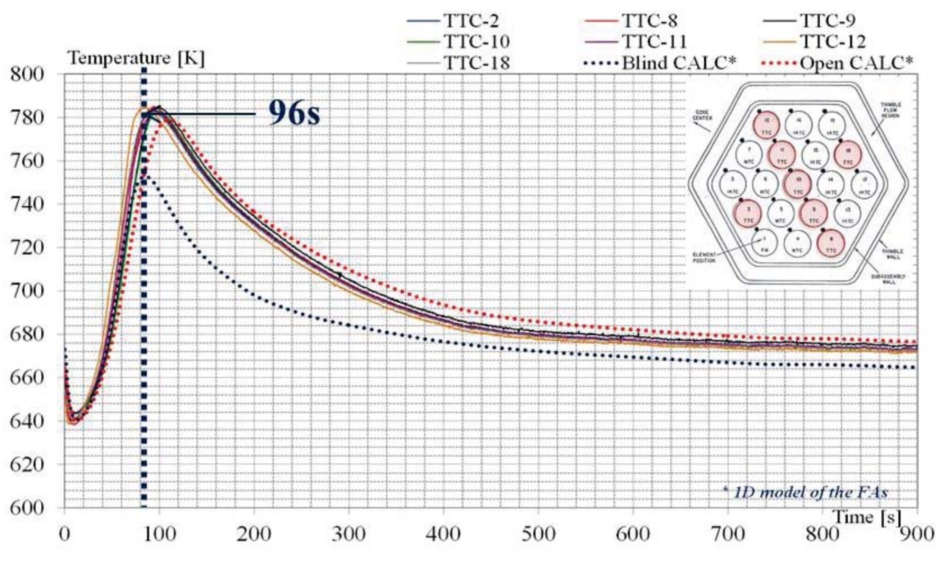


**Figure 5. XX10 cladding T at top of active core**

Considering the conduction in the coolant, it will affect the temperature distribution in the radial direction of sub-assemblies, thus influencing the temperature among the sub-channels. This level of detail is beyond the objectives of the present simulation and the capabilities of the RELAP5-3D nodalization of EBR-II. The conduction in the coolant will also affect the temperature distribution of the core bypass region. For sake of clarity, it is highlighted that the conduction of the fluid is treated as infinite, when a computational volume is concerned, and zero, when adjacent computational volumes are considered.

Considering the upper plenum of the reactor zone (see Fig. 6), the measured temperature trends are connected with the mixing, induced by the forced circulation during the phase 1 of the test, the onset of thermal stratification in phase 2, which, then, becomes the prevailing process after 100 seconds from the starting of transient. The correct prediction of the coolant thermal mixing and stratification phenomena cannot be accurately predicted by RELAP5-3D code. It is influenced by the nodalization scheme, and thus to the user effect. Improved prediction of thermal stratification can be achieved increasing the number of axial mesh in the upper plenum, and improving the knowledge of the flow paths occurring in this zone. Performances of open simulation and sensitivity analysis are reported in Fig. 6.

Phase 2 ends after about 100s, when total core power (i.e. mainly decay heat) is efficiently removed in all sub-assemblies by natural circulation flow.

During phase 3 the natural circulation is stabilized. Coolant temperature at core outlet and thermal structures in the core zone are cooled down. The results of the blind and open simulations predict correctly these trends. Improved quantitative accuracy is observed in open calculation (Tab. II), thanks to a better simulation of the natural circulation flow.

The experiment is stopped at 900s, with the coolant temperatures at sub-assemblies XX09 and XX10 equal to 691-705K and 672-675K, respectively. The blind (open) simulation predicts these temperatures 674K (700K) and 665K (676K)

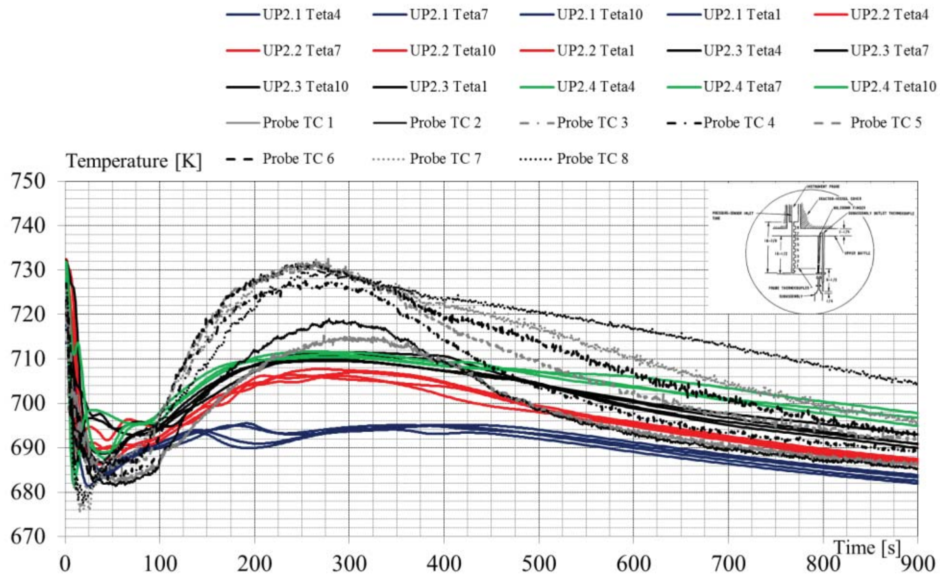


**Figure 6. Upper plenum coolant temperatures**

In summary, the blind and open simulations demonstrate RELAP5-3D has the capability to predict the main phenomena and processes relevant to safety of the test. The trends of primary mass flow rate are well predicted (open calculation). Analogous considerations are applicable to coolant and cladding temperatures of primary system. Improvements might be possible if the knowledge of EBR-II features/characteristics is improved too (e.g. inlet sub-assemblies geometry details and characterization, better understanding and quantification of the cooling induced by the IHX structures close to the Z-pipe inlet, etc…). However, some phenomena occurring in the test are challenging for the models and correlations of the code (e.g. heat structure axial conduction). Some other phenomena, such as the mixing and thermal stratification, notwithstanding simulated, are beyond RELAP5-3D capabilities and only bounding analyses are possible.

**Table I. EBR-II SHRT-17, RELAP5-3D©: steady-state comparison**

| # | Parameter | Unit | Exp | Blind Calc | Open Calc |
|---|---|---|---|---|---|
| 1 | Core Driver thermal power | MWth | 52.28 | 52.28 | 52.28 |
| 2 | Core Blanket thermal power | MWth | 5.02 | 5.02 | 5.02 |
| 3 | Core inlet temperature | K | 624.15 | 625.6 | 625.9 |
| 4 | Core outlet temperature | K | -- | 730.3 | 720.9 |
| 5 | IHX SS inlet coolant temperature | K | 574.2 | 574.2 | 574.2 |
| 6 | MCP1 mass flow rate | kg/s | 233.5 | 231.2 | 233.8 |
| 7 | MCP2 mass flow rate | kg/s | 233.2 | 230.9 | 233.8 |
| 8 | Core Driver mass flow rate | kg/s | 387.0 | 384.6 | 389.9 |
| 9 | Core Blanket mass flow rate | kg/s | 65.2 | 66.0 | 65.9 |
| 10 | IHX SS mass flow rate | kg/s | 311.4 | 311.4 | 311.4 |
| 11 | Primary pressure @ MCP out | kPa | 441.2 | 452.5 | 473.0 |
| 12 | Primary pressure @ Upper Plenum | kPa | 213.9 | 217.1 | 210.6 |

**Table II. EBR-II SHRT-17, RELAP5-3D©: imposed and resulting sequence of main events**

| Ph. W. | DESCRIPTION & PHENOMENA/PROCESSES | EVENT | Exp [s] | Blind Calc [s] | Open Calc [s] |
|---|---|---|---|---|---|
| **Phase I** (0 – 10 s) | *Pressure drop at discontinuities*<br>*Wall to fluid friction*<br>*Heat transfer in covered core*<br>*Heat transfer in passive structures and heat losses;*<br>*Pool thermal hydraulics in the tank*<br>*Multidimensional coolant temperatures and flow distributions*<br>*Heat transfer in IHX primary (i.e. bundle zone) and secondary (non-bundle) sides and between IHX primary coolant and passive structures*<br>*Thermal mixing in reactor upper plenum*<br>*Forced circulation*<br>*Pump behavior* | Stop MCP ***[Imposed]*** | 0 | 0 | 0 |
| | | Initiating event: loss of IHX flow rate ***[Imposed]*** | 0 | 0 | 0 |
| | | SCRAM ***[Imposed]*** | 0 | 0 | 0 |
| | | Min. cladding T in XX09 @ TAF | 4.5 | 4.0 | 4.0 |
| | | Min. cladding T in XX10 @ core TAF | 10 | 16 | 13 |
| | | Min. coolant T in UP | 12 | 6 | 6 |
| **Phase II** (10 – 100s) | *Pressure drop at discontinuities*<br>*Wall to fluid friction*<br>*Heat transfer in covered core*<br>*Heat transfer in passive structures and heat losses;*<br>*Pool thermal hydraulics in the tank*<br>*Multidimensional coolant temperatures and flow distributions*<br>*Conduction in fluid and structures*<br>*Heat transfer in IHX primary (i.e. bundle zone) and secondary (non-bundle) sides and between IHX primary coolant and passive structures*<br>*Thermal mixing in reactor upper plenum*<br>*Transition from forced to natural circulation*<br>*Pump behavior (i.e. coastdown)* | Max. cladding T in XX09 @ TAF | 73.5 | 67 | 81 |
| | | Max. cladding T in XX10 @ core TAF | 96.5 | 88 | 110 |
| | | Max. coolant T in UP | 138.5 | 89 | 131 |
| | | MCP 2 coastdown end [minimum of mass flow rate] | 76 | 62 | 60 |
| **Phase III** (100 – 900s) | *Pressure drop at discontinuities*<br>*Wall to fluid friction*<br>*Heat transfer in covered core*<br>*Heat transfer in passive structures and heat losses;*<br>*Pool thermal hydraulics in the tank*<br>*Multidimensional coolant temperatures and flow distributions*<br>*Conduction in fluid and structures*<br>*Heat transfer in IHX between primary coolant and passive structures*<br>*Stratification in Z-pipe*<br>*1 Φ natural circulation; and*<br>*Stratification in upper plenum* | End of transient ***[Imposed]***<br>– *(Cladding T XX09 @ TAF)*<br>– *(Cladding T XX10 @ core TAF)* | 900<br>691-705K<br>672-675K | 900<br>674K<br>665K | 900<br>700K<br>676K |

## 7. CONCLUSIONS

The activity is carried out in the framework of the IAEA CRP EBR-II Shutdown Heat Removal Tests, aimed at improving the design and the simulation capabilities in fast reactor neutronics, thermal hydraulics, plant dynamics and safety analyses. The paper presents the qualification of a three-dimensional thermal-hydraulic nodalization of EBR-II and the assessment of RELAP5-3D© code against the test SHRT-17.

The analysis of results demonstrates that RELAP5-3D© code has the capability to predict the main phenomena and processes relevant to safety of test SHRT-17. In particular,

- The trends of mass flow rate, of coolant and cladding temperatures in the core are well predicted (open calculation).
- Improvements might be possible if the knowledge of EBR-II features/characteristics is improved too (e.g. inlet sub-assemblies geometry details and characterization, better understanding and quantification of the cooling induced by the IHX structures close to the Z-pipe inlet, etc…).
- The axial conduction in the structure is challenging for the code.
- Mixing and thermal stratification, notwithstanding simulated, are beyond RELAP5-3D capabilities and only bounding analyses are possible.

In conclusion, the availability of the experimental data and the present benchmarking activity brought to the following achievements.

- The experiment SHRT-17 provides unique and fundamental experimental data for maintaining the competences in the field of fast reactors, as well as for supporting the design and the safety analysis of Gen. IV liquid metal fast reactors.
- The availability of the experimental data represent a valuable extension of the experimental database for code validation.
- The RELAP5-3D© simulation of the test is an enlargement of the independent validation activity on the code.

## ACKNOWLEDGMENTS

The present activity was carried out with the economic support of the Italian Ministry of Industry and Economic Development. The authors acknowledge IAEA and S. Monti for promoting, managing and supporting the coordinated research project (CRP) on EBR-II Shutdown Heat Removal Tests (SHRT). Acknowledgements to Argonne National Labs for delivering the experimental data of EBR-II tests SHRT17 and SHRT45r to IAEA and the benchmark participants.

## REFERENCES

1. L. BRIGGS et al., “Benchmark analyses of the Shutdown Heat Removal Tests Performed in the EBR-II Reactor”.
2. A. Del Nevo, C. Venturi, E. Martelli, D. Rozzia, “Qualifica di codici di calcolo dedicati alle analisi di sistema avanzati quando applicati nella simulazione di impianti a metallo liquido”, ENEA, ADPFISS-LP2-039, 24 Settembre 2013.
3. A. Del Nevo, E. Martelli et al. , “Development and validation of an approach and numerical models for safety analysis of FBR”, ENEA, ADPFISS-LP2-039.
4. A. Del Nevo, K. Umminger, “Integral test facility and thermal-hydraulic system codes in nuclear safety analysis”, Science and Technology of Nuclear Installations, 2012.
5. J.-Y. DORIATH, ET AL., "ERANOS1: The Advanced European System of Codes for Reactor Physics", International Conference on Mathematical Methods and Supercomputing in Nuclear Applications, Karlsruhe, Germany, 1993.
6. T. Goorley et al., “Initial MCNP6 Release Overview,” LA-UR-11-05198, Los Alamos National Laboratory, USA.
7. SCALE-4.4a: A Modular Code System for Performing Standardized Computer Analyses for Licensing Evaluation, ORNL/NUREG-CR-0200, Rev. 6, Oak Ridge National Laboratory (March 2000).
8. C. Rabiti, Y. Wang, G. Palmiotti, H. Hiruta, J. Cogliati, A. Alfonsi “PHISICS: a New Reactor Physics Analysis Toolkit,” Proceedings American Nuclear Society 2011 Annual Meeting, Hollywood, Florida, USA, June 27-30 (2011).
9. ANSYS CFX Release 13 User Manual, 2011.

10. K. Lassmann, A. Schubert, P. Van Uffelen, C. Gyory, and J. van de Laar, "Transuranus Handbook" version v1m1j06, JRC, EC, ITU, 2006.
11. T. Sumner and T.Y.C. Wei, "Benchmark Specifications and data Requirements for EBR-II Shutdown Heat Removal tests SHRT-17 and SHRT-45R", ANL-ARC-226 (rev 1), May 31, 2012.
12. INL, "RELAP5-3D© Code Manual Volume II: User's Guide and Input Requirements", INEEL-EXT-98-00834, Revision 4.0, June 2012.
13. E. Martelli, Thermal-hydraulic transient analysis of a loss-of-flow accident in the EBR-II SFR, using RELAP5-3D computer program, M.S. thesis, Sapienza University of Rome, Italy, 2014.
14. C.B. Davis, Applicability of RELAP5-3D for Thermal-Hydraulic Analyses of a Sodium-Cooled Actinide Burner Test Reactor, INL/EXT-06-11518, July 2006.
15. E.H. Novendstern, Turbulent Flow pressure drop model for fuel rod assemblies utilizing a helical wire-wrap spacer system, Nucl. Eng. Des., 22, pp. 19-27, 1972.
16. C.B. Davis, "Evaluation of the Use of Existing RELAP5-3D Models to Represent the Actinide Burner Test Reactor", INL/EXT-07-12228, February 2007.
17. N. E. Todreas and M. S. Kazimi, Nuclear Systems I: Thermal Hydraulic Fundamentals, Washington DC: Hemisphere, 1990.